

UCRL-CONF-215092

LAWRENCE  
LIVERMORE  
NATIONAL  
LABORATORY

# Laser coupling to reduced-scale targets at NIF Early Light

D. E. Hinkel, M. B. Schneider, B. K. Young, J. P. Holder, A. B. Langdon, H. A. Baldis, G. Bonanno, D. E. Bower, H. C. Bruns, K. M. Campbell, J. R. Celeste, S. Compton, R. L. Costa, E. L. Dewald, S. N. Dixit, M. J. Eckart, D. C Eder, M. J. Edwards, A. D. Ellis, J. A. Emig, D. H. Froula, S. H. Glenzer, D. Hargrove, C. A. Haynam, R. F. Heeter, M. A. Henesian, G. Holtmeier, D. L. James, K. S. Jancaitis, D. H. Kalantar, J. H. Kamperschroer, R. L. Kauffman, J. Kimbrough, R. K. Kirkwood, A. E. Koniges, O. L. Landen, M. Landon, F. D. Lee, B. J. MacGowan, A. J. Mackinnon, K. R. Manes, C. Marshall, M. J. May, J. W. McDonald, J. Menapace, S. E. I. Moses, D. H. Munro, J. R. Murray, C. Niemann, D. Pellinen, G. D. Power, V. Rekow, J. A. Ruppe, J. Schein, R. Shepherd, M. S. Singh, P.T. Springer, C. H. Still, L. J. Suter, et al.

September 6, 2005

International Conference on Inertial Fusion Science  
Barritz, France  
September 4, 2005 through September 9, 2005

## **Disclaimer**

---

This document was prepared as an account of work sponsored by an agency of the United States Government. Neither the United States Government nor the University of California nor any of their employees, makes any warranty, express or implied, or assumes any legal liability or responsibility for the accuracy, completeness, or usefulness of any information, apparatus, product, or process disclosed, or represents that its use would not infringe privately owned rights. Reference herein to any specific commercial product, process, or service by trade name, trademark, manufacturer, or otherwise, does not necessarily constitute or imply its endorsement, recommendation, or favoring by the United States Government or the University of California. The views and opinions of authors expressed herein do not necessarily state or reflect those of the United States Government or the University of California, and shall not be used for advertising or product endorsement purposes.

The headers will be insert by the Publisher  
The headers will be insert by the Publisher  
The headers will be insert by the Publisher

## Laser coupling to reduced-scale targets at NIF Early Light

D. E. Hinkel<sup>1</sup>, M. B. Schneider<sup>1</sup>, B. K. Young<sup>1</sup>, J. P. Holder<sup>1</sup>, A. B. Langdon<sup>1</sup>, H. A. Baldis<sup>2</sup>, G. Bonanno<sup>1</sup>, D. E. Bower<sup>1</sup>, H. C. Bruns<sup>1</sup>, K. M. Campbell<sup>1</sup>, J. R. Celeste<sup>1</sup>, S. Compton<sup>1</sup>, R. L. Costa<sup>1</sup>, E. L. Dewald<sup>1</sup>, S. N. Dixit<sup>1</sup>, M. J. Eckart<sup>1</sup>, D. C Eder<sup>1</sup>, M. J. Edwards<sup>1</sup>, A. D. Ellis<sup>1</sup>, J. A. Emig<sup>1</sup>, D. H. Froula<sup>1</sup>, S. H. Glenzer<sup>1</sup>, D. Hargrove<sup>1</sup>, C. A. Haynam<sup>1</sup>, R. F. Heeter<sup>1</sup>, M. A. Henesian<sup>1</sup>, G. Holtmeier<sup>1</sup>, D. L. James<sup>1</sup>, K. S. Jancaitis<sup>1</sup>, D. H. Kalantar<sup>1</sup>, J. H. Kamperschroer<sup>1</sup>, R. L. Kauffman<sup>1</sup>, J. Kimbrough<sup>1</sup>, R. K. Kirkwood<sup>1</sup>, A. E. Koniges<sup>1</sup>, O. L. Landen<sup>1</sup>, M. Landon<sup>1</sup>, F. D. Lee<sup>1</sup>, B. J. MacGowan<sup>1</sup>, A. J. Mackinnon<sup>1</sup>, K. R. Manes<sup>1</sup>, C. Marshall<sup>1</sup>, M. J. May<sup>1</sup>, J. W. McDonald<sup>1</sup>, J. Menapace<sup>1</sup>, S. E. I. Moses<sup>1</sup>, D. H. Munro<sup>1</sup>, J. R. Murray<sup>1</sup>, C. Niemann<sup>1</sup>, D. Pellinen<sup>3</sup>, G. D. Power<sup>1</sup>, V. Rekow<sup>1</sup>, J. A. Ruppe<sup>1</sup>, J. Schein<sup>1</sup>, R. Shepherd<sup>1</sup>, M. S. Singh<sup>1</sup>, P.T. Springer<sup>1</sup>, C. H. Still<sup>1</sup>, L. J. Suter<sup>1</sup>, G. L. Tietbohl<sup>1</sup>, R. E. Turner<sup>1</sup>, B. M. VanWonterghem<sup>1</sup>, R. J. Wallace<sup>1</sup>, A. Warrick<sup>1</sup>, P. Watts<sup>3</sup>, F. Weber<sup>1</sup>, P. J. Wegner<sup>1</sup>, E. A. Williams<sup>1</sup>, P. E. Young<sup>1</sup>

<sup>1</sup>Lawrence Livermore National Laboratory, 7000 East Avenue, Livermore, CA 94550

<sup>2</sup>University of California at Davis, One Shields Avenue, Davis, CA 95616, USA

<sup>3</sup>Bechtel Nevada Corporation, Livermore, CA, USA 94550

**Abstract.** Deposition of maximum laser energy into a small, high-Z enclosure in a short laser pulse creates a hot environment. Such targets were recently included in an experimental campaign using the first four of the 192 beams of the National Ignition Facility [J. A. Paisner, E. M. Campbell, and W. J. Hogan, *Fusion Technology* **26**, 755 (1994)], under construction at the University of California Lawrence Livermore National Laboratory. These targets demonstrate good laser coupling, reaching a radiation temperature of 340 eV. In addition, the Raman backscatter spectrum contains features consistent with Brillouin backscatter of Raman forward scatter [A. B. Langdon and D. E. Hinkel, *Physical Review Letters* **89**, 015003 (2002)]. Also, NIF Early Light diagnostics indicate that 20% of the direct backscatter from these reduced-scale targets is in the polarization orthogonal to that of the incident light.

### 1. Introduction

A platform for analysis of material properties under extreme conditions, where a sample is bathed in radiation with a high temperature, is under development. This platform is a high-Z enclosure just large enough for incident laser beams to gain entrance. The beams strike its interior, and the absorbed laser energy is re-emitted as x-radiation, which fills the enclosure. The construction of high-power lasers such as the National Ignition Facility (NIF)[1] at the University of California Lawrence

Livermore National Laboratory (LLNL) in the U.S.A. and the Laser MegaJoule[2] in France provides the necessary energy to drive these targets in the high energy density regime.

Such reduced-scale targets were recently included in an experimental campaign using the first four of the 192 laser beams of NIF[3,4], and similar investigations[4,5] have been performed at University of Rochester's Omega laser in the U.S.A. These targets perform in a regime of high laser intensity, electron density, and electron temperature, where laser-target coupling may be compromised. This investigation provides information on optimizing target size as a function of laser performance and furthers the mitigation of laser-plasma interactions (LPI) under such conditions.

In this paper we present results on laser-target coupling in these small cans. Such coupling is limited by ablated wall material, which fills the target during the laser pulse. It is further limited by laser backscatter. Finally, if laser beam filamentation *outside* of the target produces a laser beam with a spot size larger than the laser entrance hole (LEH), filamentation can also limit laser-target coupling. [Filamentation occurs when the laser interacts with density perturbations, ponderomotively creating density depressions into which the beam refracts, further driving the density depression.]

Our primary findings are as follows. Radiation temperatures as high as 340 eV were achieved with approximately 9.5 kJ of laser energy incident into a gold can with a diameter (and LEH) of 560  $\mu\text{m}$  and a length of 525  $\mu\text{m}$ . There was approximately 15% backscatter of which  $> 11\%$  was stimulated Brillouin backscatter (SBS, where incident laser light backscatters off forward-propagating ion acoustic waves) and  $< 4\%$  was stimulated Raman backscatter (SRS, where incident light backscatters off forward-propagating electron plasma waves). SRS at high intensity and with maximum conditioning of the incident beams is consistent with Raman re-scatter[6], where Raman forward scattered light (SRFS, where incident light forward scatters off an electron plasma wave) itself undergoes SBS. There is evidence of strong filamentation, as  $\sim 65 - 70\%$  of the backscatter is on the NBI plate. Finally, in laser shots where the laser light was linearly polarized, approximately 20% of the backscatter was in the polarization orthogonal to the incident light. These findings were made possible by NIF's state-of-the-art diagnostic capability.

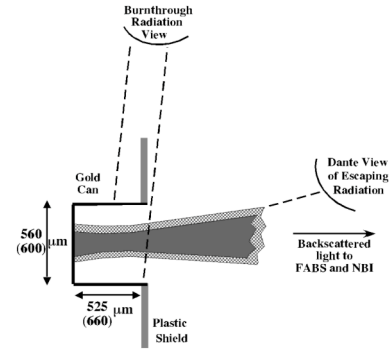
## 2. The Experiment

The four NIF laser beams (NIF Early Light, or NEL) have been commissioned to target chamber center, entering the target chamber from the bottom left. For these reduced-scale targets, the beams were conditioned with small-spot phase plates, and with polarization smoothing[3], thereby reducing the amount of power at high intensity while keeping the spot small enough to enter the target. Dante[7], an absolutely calibrated, time-resolved x-ray spectrometer collects x-radiation from the laser entrance hole at an angle of  $21.8^\circ$  with respect to the target axis. Direct laser backscatter is spectrally and temporally resolved with the full-aperture backscatter station (FABS)[8]. The early near-backscatter imager (eNBI)[9] is located across the target chamber from the beam ports, and images the scattered laser light collected on a plate surrounding the beam ports. Timed-pinhole images of these thin-walled (3.5  $\mu\text{m}$  thickness) targets were collected at an  $84^\circ$  angle with respect to the target axis, and these results are presented in Ref. [4] at this IFSA 2005 conference. Large, lead-doped, plastic shields surround the gold can at the laser entrance hole so that Dante views only the x-ray flux emitted through the laser entrance hole. The target geometry is summarized in Figure 1.

We report here on five reduced-scale targets shot at NEL. All use a 1.1 ns (FWHM) square pulse and small-spot phase plates[3]. The first three shots also employ polarization smoothing. Shot One has 6.12 kJ of laser energy entering a target 560  $\mu\text{m}$  in diameter and 525  $\mu\text{m}$  in length. Shot Two uses the

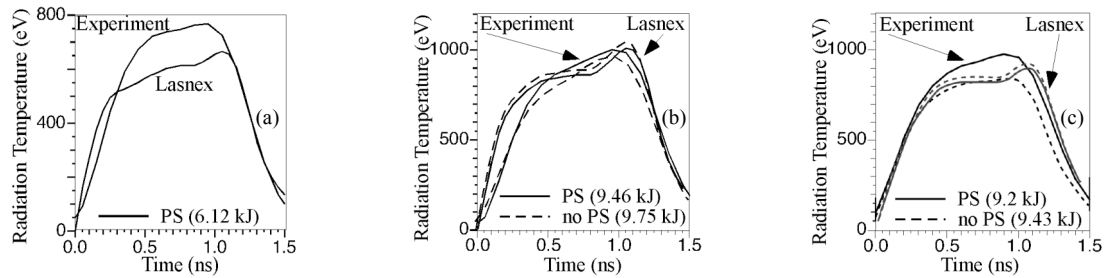
same target, but is at a higher energy of 9.46 kJ. Shot Three, at an energy of 9.2 kJ, is into a target 600  $\mu\text{m}$  in diameter can and 660  $\mu\text{m}$  in length. Finally, Shots Four and Five are repeats of Shots Two and Three at energies of 9.75 and 9.43 kJ, respectively, but without polarization smoothing.

**Figure 1.** Target geometry for reduced-scale targets at NEL. Four laser beams are incident on the back wall of a gold can, along the target axis. X-radiation leaving the can is collected at an angle of  $21^\circ$ , and burnthrough radiation is collected through the 3.5  $\mu\text{m}$  thick side walls at  $84^\circ$  relative to the target axis. The backscatter is collected by FABS and NBI. The targets were either 600  $\mu\text{m}$  in diameter and 660  $\mu\text{m}$  in length, or 560  $\mu\text{m}$  in diameter and 525  $\mu\text{m}$  in length. The aspect ratio of the two targets is purposefully different, making the latter target more extreme.



### 3. Results

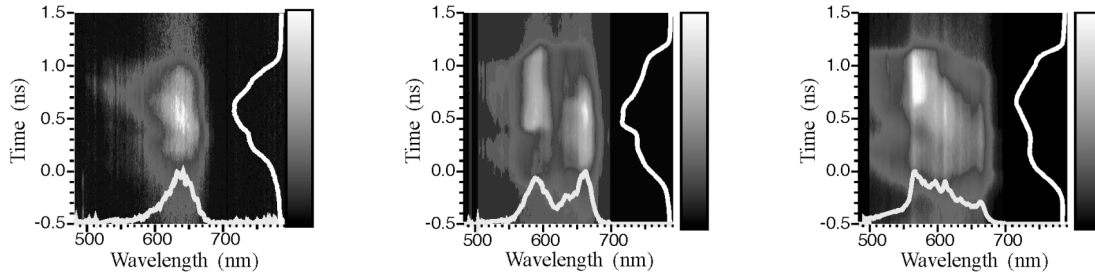
Figures 2 summarize the Dante results, where measured radiation flux versus time is presented and compared to the Lasnex simulations which account for 10% backscatter with a temporal profile consistent with the measured SBS.



**Figures 2.** Measured and simulated radiation flux for the five reduced-scale targets shot at NEL: (a) Shot One at 6.12 kJ into the 560  $\mu\text{m}$  diameter can ( $T_r = 318$  eV) -- Lasnex simulations calculate a lower level of flux than is measured in experiment, resulting in a  $T_r = 307$  eV; (b) Shots Two (9.46 kJ) and Four (9.75 kJ), with and without polarization smoothing into the 560  $\mu\text{m}$  diameter can -- Shot Two reaches a  $T_r = 340$  eV, as does the Lasnex simulation, whereas Shot Four at slightly higher energy resulted in  $T_r = 337$  eV with a Lasnex prediction of 343 eV; (c) Shots Three (9.2 kJ) and Five (9.43 kJ), with and without polarization smoothing into the 600  $\mu\text{m}$  diameter can -- Shot Three reaches a  $T_r = 327$  eV, whereas Lasnex predicts a  $T_r = 320$  eV; Shot Five has a peak  $T_r = 315$  eV, but the Lasnex simulation calculates  $T_r = 322$  eV.

This target size scaling provides information about the efficiency of laser-target coupling. The energy coupling at high energy (cf. Figure 2b) is only 80% of that in the low energy shot (cf. Figure 2a). This suggests that even with polarization smoothing, beam spray is limiting coupling, as the fractional backscatter is nearly identical. Lasnex underpredicts the radiation flux, perhaps because it is overestimating target fill. The inclusion of azimuthal hydrodynamic magnetic fields could act to confine the heat conduction to roughly the laser spot size, thereby reducing target filling. An improved opacity model simulation would potentially alter the target filling as well. These are challenging simulations to perform, but nonetheless are currently being pursued.

Figures 3 depict the Raman spectra, which contain information about the electron density ( $n_e$ ) and temperature ( $T_e$ ) at which scatter occurs. Figure 3a is a plot of the Raman backscatter for Shot One. The spectrum peaks in wavelength at  $\sim 640$  nm, or at  $n_e = 0.14 n_c$  (where  $n_c$  is the critical density for light of wavelength 0.351  $\mu\text{m}$ ),  $T_e = 7$  keV. The higher energy shot with polarization smoothing (Figure 3b) shows evidence of two peaks. This could be SRS occurring at two different places in the target, but late in time, SRS can only occur along a density gradient outside the target, which is not consistent with such a scenario. Another possibility is that Raman backscatter occurs at 660 nm, but that the peak at 590 nm is Brillouin backscatter of Raman forward scatter[6]. Finally the higher energy shot without polarization smoothing (Figure 3c) shows evidence of filamentation, as SRS, occurring along a density gradient outside the target, is occurring at a lower density as time increases.



**Figures 3.** Raman spectra for (a) Shot One, at 6.12 kJ with polarization smoothing; (b) Shot Two, at 9.46 kJ with polarization smoothing; (c) Shot Four, at 9.75 kJ without polarization smoothing. Shot Two has a Raman spectrum consistent with Raman re-scatter, where the peak at 660 nm is SRS, and that at 590 nm is SBS of SRFS. Shot Four provides evidence that filamentation occurs without polarization smoothing.

The experiments presented in this paper highlight the unique characteristics of reduced-scale targets shot at NEL. These targets emit a radiation flux of  $\sim 1000$  GW/sr, exhibit features in the Raman spectrum consistent with re-scatter of Raman forward scatter, and show de-polarization of polarized incident light, presumably caused by magnetic fields. These experiments have challenged our current state-of-the-art simulations, and will ultimately enhance our predictive capability.

### Acknowledgments

We thank the NIF and OMEGA staff for their expertise and hard work. This work was performed under the auspices of the U.S. Department of Energy by the University of California Lawrence Livermore National Laboratory under Contract No. W-7405-ENG-48.

### References

- [1] J. A. Paisner, E. M. Campbell, and W. J. Hogan, *Fusion Technology* **26**, 755 (1994).
- [2] M. L. Andre, *Proc. SPIE Int. Soc. Opt. Eng.* **3047**, 38 (1997).
- [3] D. E. Hinkel, M. B. Schneider, H. A. Baldis, *et al.*, *Phys. Plasmas*, **12**, 056305, (2005)
- [4] M. B. Schneider *et al.*, in *Proceedings of the Fourth International Conference on Inertial Fusion Sciences and Applications, Biarritz, France, 2005 (to be published)*.
- [5] H.A. Baldis, C.G. Constantin, M.B. Schneider *et al.*, in *Proceedings of the Fourth International Conference on Inertial Fusion Sciences and Applications, Biarritz, France, 2005 (to be published)*.
- [6] A.B. Langdon and D.E. Hinkel, *Phys. Rev. Lett.* **89**, 015003 (2002).
- [7] E. L. Dewald, K. M. Campbell, R. E. Turner *et al.*, *Rev. Sci. Inst.* **75**, 3759 (2004).
- [8] D. H. Froula, D. Bower, M. Christ *et al.*, *Rev. Sci. Inst.* **75**, 4168 (2004); R. K. Kirkwood, T. McCarville, D. H. Froula *et al.*, *Rev. Sci. Inst.* **75**, 4175 (2004); D. E. Bower, T. J. McCarville, S. S. Alvarez *et al.*, *Rev. Sci. Inst.* **75**, 4177 (2004).
- [9] A. J. Mackinnon, T. McCarville, K. Piston *et al.*, *Rev. Sci. Inst.* **75**, 4183 (2004).